

Article

# Impact of Blockage Ratio on Thermal Performance of Delta-Winglet Vortex Generators

Indri Yaningsih<sup>1,2,3,\*</sup> , Agung Tri Wijayanta<sup>2,\*</sup>, Takahiko Miyazaki<sup>1,3</sup> and Shigeru Koyama<sup>1,3</sup>

<sup>1</sup> Department of Energy and Environmental Engineering, Interdisciplinary Graduate School of Engineering Sciences, Kyushu University, 6-1 Kasuga-koen, Kasuga-shi, Fukuoka 816-8580, Japan; miyazaki.takahiko.735@m.kyushu-u.ac.jp (T.M.); koyama@phase.cm.kyushu-u.ac.jp (S.K.)

<sup>2</sup> Department of Mechanical Engineering, Faculty of Engineering, Sebelas Maret University, Jl. Ir. Sutami 36 A, Surakarta 57126, Indonesia

<sup>3</sup> Thermal Science and Engineering Division, International Institute of Carbon-Neutral Energy Research (I2CNER), Kyushu University, 744 Motooka, Nishi-ku, Fukuoka 819-0395, Japan

\* Correspondence: 3es17301g@s.kyushu-u.ac.jp (I.Y.); agungtw@uns.ac.id (A.T.W.); Tel.: +81-925-837-832 (I.Y.)

Received: 29 December 2017; Accepted: 24 January 2018; Published: 26 January 2018

**Abstract:** The impact of double-sided delta-winglet tape (DWTs) inserts on convective heat transfer and friction behaviors in a tube was experimentally investigated. Three DWTs with ratios of winglet-height ( $b$ ) to inner tube diameter ( $d_i$ ) called blockage ratio ( $R_b$ ) of 0.28, 0.35 and 0.42 were tested and their performance was compared to that of a longitudinal strip and plain tube under similar test flow conditions. Experiments were conducted over a wide range of flow rates,  $3.35 \times 10^{-5}$ – $8.33 \times 10^{-5}$  m<sup>3</sup>/s, which correspond to  $5500 \leq$  Reynolds number ( $Re$ )  $\leq 14,500$  in the 14.3 mm i.d. tube. The results revealed that using DWTs dramatically increased the Nusselt number ( $Nu$ ) by as much as 364.3% and the friction factor ( $f$ ) by 15.5 times compared with those of a plain tube. Thermal performance ( $\eta$ ) increased with a corresponding increase in  $R_b$ . The highest thermal performance ( $\eta$ ) obtained was 1.4. Showing a notable improvement on the thermal performance of the system, DWTs are proposed as a favorable insert device.

**Keywords:** blockage ratio; delta winglet; vortex generator; friction factor; Nusselt number

## 1. Introduction

Vortex generators (VGs) have received extensive attention by researchers [1–5] as devices for obtaining high thermal performance by enhancing the heat-transfer coefficients of a tube heat exchanger. VGs are also regarded as potential heat-transfer augmentation devices because they create vortices that lead to high heat-transfer rates [5]. VGs are used to induce secondary flow, which disturbs or cuts off the thermal boundary layer developed along the wall and removes heat from the wall to the core of the flow by means of large-scale turbulence [6]. VGs that form longitudinal vortices are extremely attractive because they experience only a small pressure drop penalty. These longitudinal vortices can be generated by using wing or winglet type VGs, which create flow separation at the leading edge of the wing [7]. Generally, wing/winglet type VGs function like a fin and are fabricated by punching out or mounting onto a strip/base fin. Considerable improvements in convective heat transfer using the wing/winglet VGs have been demonstrated [8–15]. An experimental and numerical study on a rectangular channel fitted with a delta-winglet vortex generator was conducted by Wu and Tao [8]. The attack angles were varied ( $15^\circ$ ,  $30^\circ$ ,  $45^\circ$ , and  $60^\circ$ ) to obtain an optimum heat-transfer profile for the channel. A large attack angle was found to exhibit a high heat-transfer rate, which was due to a disruption of the air flow in the lower channel by the transverse flow through the punched holes. He et al. [9] also conducted a numerical study on heat-transfer augmentation by investigating the mechanism of the flow structure. Variation in the attack angle, row number, and placement of

rectangular winglet pairs was discussed in detail. They found that by altering the position of the winglet, pressure drop could be reduced without decreasing heat transfer.

The effect of variations in the profile of rectangular winglets (i.e., wavy-up and wavy-down) on the heat-transfer performance of a fin-and-tube heat exchanger was numerically investigated and compared with that of a conventional rectangular channel without a winglet by Gholami et al. [10]. The wavy-up and wavy-down rectangular winglets were found to exhibit better heat-transfer performance. Moreover, the effect of the wavy-up configuration was more significant than the wavy-down configuration. Khoshvaght-Aliabadi et al. [11] experimentally studied the influence of various delta-winglet arrangements (one side cut with one delta-winglet, one side cut with two delta winglets, two sides cut with two delta winglets, and two sides cut with four delta winglets) on the heat-transfer augmentation of a tube and compared that to the performance of a plain tube. The results showed that a tube with delta winglets had better thermal performance than a plain tube, and that the arrangements of two sides cut with four delta winglets outperformed all other arrangements.

A combined winglet pair (a rectangular wing and a trapezoidal wing) proposed as a novel longitudinal VG was numerically investigated by Wang et al. [12]. Compared with a rectangular winglet pair, the combined winglet pair showed considerable improvement in heat transfer with a moderate pressure drop penalty. Abdollahi and Shams [13] numerically studied the optimization parameters (shape and attack angle) of a winglet VG. They showed that at low Reynolds number, attack angle modification did not significantly improve performance; in contrast, for a high Reynolds number, variation in the attack angle considerably influenced performance because the angle could increase drag. Moreover, among the different VG shapes (traditional vortex generator, delta vortex generator, rectangular vortex generator, and trapezoidal vortex generator), the rectangular vortex generator was found to provide the best heat-transfer performance because it had a large facing flow area. The effect of a combined wavy-groove and delta-winglet VG on the thermal performance of a solar air heater channel was experimentally investigated by Skullong et al. [14]. Experiments were conducted at a constant wing attack angle with three different wing porosity area ratios and four groove-wing distance to channel-height ratios. The different parametric combinations exhibited different behaviors in the thermal performance of the system. Sarangi and Mishra [15] numerically examined the influence of the winglet position on the heat-transfer characteristics of a fin-and-tube heat exchanger. They found that an increase in the number of winglets enhanced the heat-transfer rate. In addition, the position of the delta winglet at the center of the tube showed more efficient heat transference than delta winglet in inlet and exit of heat exchanger.

The above studies have demonstrated that VGs with a delta wing/winglet are promising as heat exchanging devices. However, there are several issues related to an acceptable friction factor that still need to be addressed. The enhancement of the heat-transfer area with delta wing/winglet can be achieved by modifying the shapes of the delta wing/winglet (triangular, rectangular, or spherical), geometrical structures (the attack angle, winglet width, and winglet height), fluid flow directions (forward and backward), and flow parameters. The performance of the heat exchanger can be significantly improved by changing the important parameters of the insertion. The delta wing/winglets are mostly used to increase the convective heat transfer in gas to gas heat exchangers. In this work, the VGs are installed in liquid to liquid heat exchanger to cover the application by using the different of working fluids. This present study is a continuation of our previous work [16]. Modification of the geometrical structure of the double-sided delta-winglet tape (DWT) VGs in term of attack angle has been experimentally examined. Founded on earlier work, a significant improvement of the heat-transfer coefficient could be achieved by using a large attack angle of  $70^\circ$ . Hence, to optimize the thermal performance of the heat exchanger, the high attack angle is also adopted in the current study. The present investigation develops the application of double-sided DWT VGs to obtain the convective heat-transfer and friction factor behaviors in a tube. Additionally, the important parameters from the data obtained are employed to invent the empirical correlations for the Nusselt number, friction factor, and thermal performance factor.

## 2. Materials and Methods

### 2.1. Experimental Setup

The present study examines the effect of double-sided DWT VGs having varying values of blockage ratio ( $R_b$ ) on convective heat-transfer behaviors and compares the results of using DWTs with those using plain tubes and a tube with a longitudinal strip (LS) without a wing. Experiments were performed with values of Reynolds number ( $Re$ ) ranging from 5500 to 14,500. A schematic diagram of the enhanced heat-transfer test rig is shown in Figure 1. Convective heat-transfer behaviors were evaluated by employing a horizontal concentric tube heat exchanger as the test section.

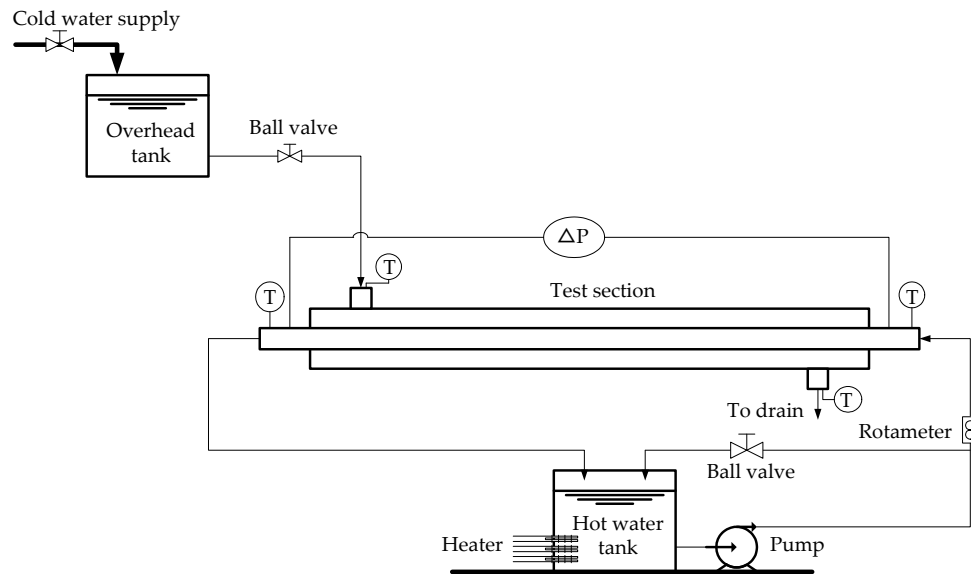
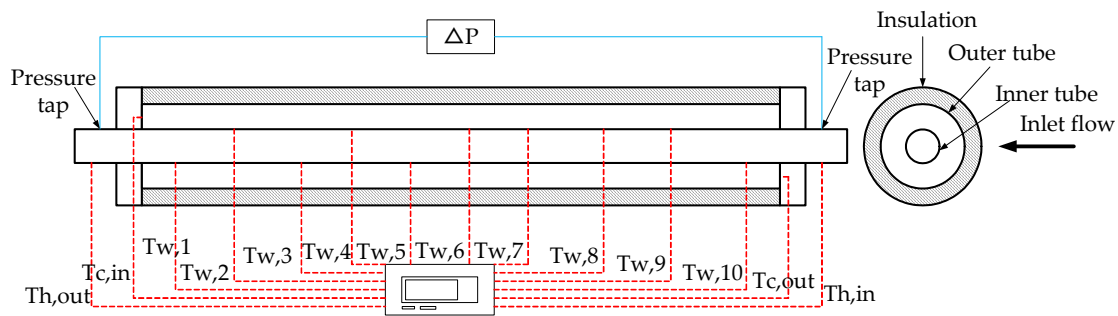


Figure 1. Schematic diagram of the enhanced heat-transfer setup.

The horizontal concentric tube heat exchanger was fabricated from aluminum and comprised an inner tube with a length ( $L_i$ ) of 2500 mm and an inner diameter ( $d_i$ ) of 14.3 mm and an outer tube with a length ( $L_o$ ) of 1950 mm and an inner diameter ( $D_i$ ) of 23.4 mm. Two working fluids were used in the system: cold water for the outer tube and hot water for the inner tube with both liquids flowing in the counter-current direction. The cold water stream moved through an open loop system such that cold water was circulated once through the system and then discharged out into the environment. In contrast, the hot water stream moved through a closed loop system that recycled and recirculated the hot water. The mass flow rate was varied by regulating the rotameter within the accuracy of  $\pm 0.5\%$  of Reading (RD). During the experiments, hot water was held at a constant temperature of  $60\text{ }^\circ\text{C}$  with a varied flow rate ranging from 0.033 to 0.099 kg/s. To ensure a supply of hot water, an electric heater was utilized to control the temperature of water within a range of  $\pm 0.1\text{ K}$  [17]. Cold water constantly flowed at 0.103 kg/s at an ambient temperature of  $28\text{ }^\circ\text{C}$ . A glass wool covering was used to insulate the outside of the heat exchanger.

To investigate heat transfer and friction factor behaviors, temperature and pressure were measured. Figure 2 is a schematic of the heat-transfer test section with measurement points along the test section for registering temperature and pressure. Fourteen K-type thermocouples with an accuracy of  $\pm 0.1\text{ K}$  (three-point calibration) were embedded in the test section: two thermocouples measured the inlet and outlet temperature of the inner tube; two thermocouples measured the inlet and outlet temperature of the outer tube; and ten thermocouples were positioned on the outer wall of the inner tube. Pressure differences were determined using a U-tube manometer filled with water. To ensure measurement accuracy, four pressure taps were mounted on the inlet and outlet of the inner tube.



**Figure 2.** Schematic diagram of the enhanced heat-transfer test section with measurement points for registering temperature and pressure.

DWTs and LSs were fabricated using aluminum with the following dimensions: 0.7 mm in thickness, 12.6 mm in width ( $W$ ), and 2000 mm in length ( $L$ ). The DWTs are a modification of the LS with winglets punched out at the vertical center of the strip and made to protrude either upward or downward in an alternating fashion at a certain attack angle with respect to the strip base. When the winglet is punched out, it will create an attack angle between the wing/winglet with the remaining strip/base fin. Based on our previous study [16], the values of the attack angle ( $\alpha = 70^\circ$ ), winglet-pitch ( $p = 15$  mm), and winglet width ( $c = 8$  mm) were kept constant. The winglet heights ( $b$ ) of the DWTs were 4, 5, and 6 mm, giving a blockage ratio ( $R_b = b/d_i$ ) of 0.28, 0.35, and 0.42, respectively. DWTs were made across the entire strip. Details of the DWTs are shown in Figure 3.

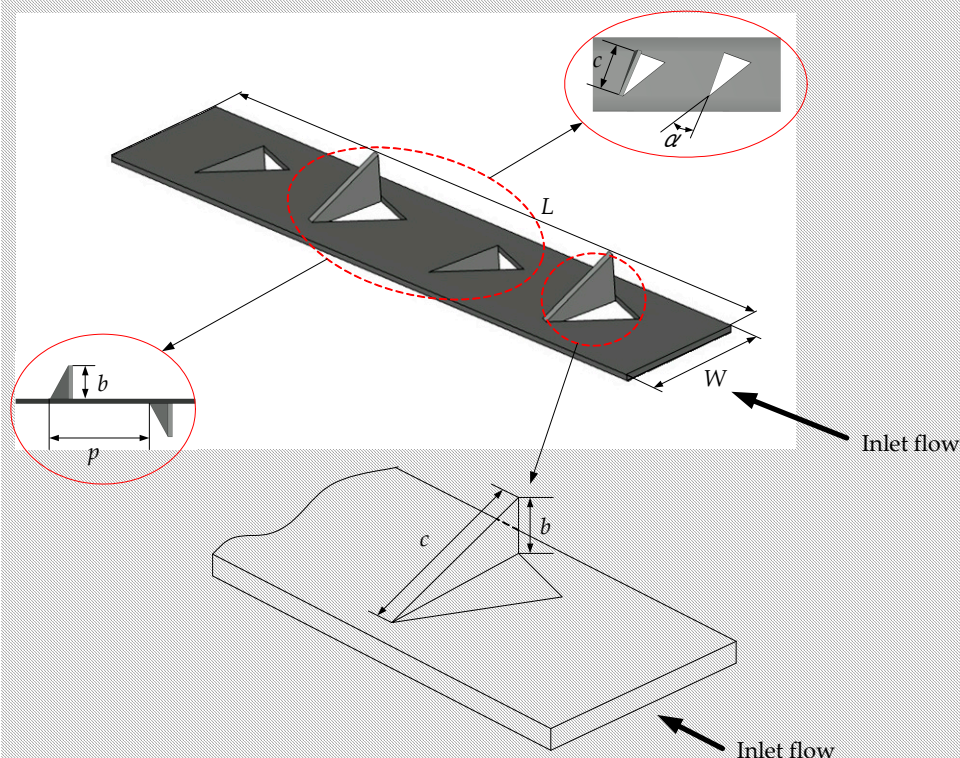


**Figure 3.** Schematic diagram of double-sided delta-winglet vortex generators.

### 2.2. Data Reduction Equations

Data reduction details for analyzing the experimental data are provided below. The experimental data covered the wide range of Reynolds number (from 5500 to 14,500). Heat-transfer and fluid-flow characteristics were expressed as non-dimensional parameters, i.e., Nusselt number ( $Nu$ ) and friction

factor ( $f$ ), respectively. When the steady state condition was achieved, temperature and pressure readings were obtained. For each variation in the test condition at least 18 data points were collected. Certain properties of water were characterized according to the thermo-physical properties of water at the bulk mean temperature.

The heat-transfer rate of the cold water on the outer side of the tube ( $Q_c$ ) was given as

$$Q_c = \dot{m}_c c_{p,c} (T_{c,o} - T_{c,i}) = h_o A_o (\bar{T}_{w,o} - T_{b,c}). \quad (1)$$

$T_{w,o}$  referred to the mean outer wall temperature of the inner tube and was calculated as

$$\bar{T}_{w,o} = \frac{\sum T_{w,o}}{10}. \quad (2)$$

$T_{b,c}$  referred to the bulk cold water temperature and was calculated as

$$T_{b,c} = \frac{T_{c,i} + T_{c,o}}{2}. \quad (3)$$

The heat-transfer rate of the hot water in the inner tube side ( $Q_h$ ) was evaluated as

$$Q_h = \dot{m}_h c_{p,h} (T_{h,i} - T_{h,o}) = U_i A_i \Delta T_{LMTD}. \quad (4)$$

$\Delta T_{LMTD}$  referred to the logarithmic mean temperature difference and was calculated according to the following equation:

$$\Delta T_{LMTD} = \frac{(T_{h,i} - T_{c,o}) - (T_{h,o} - T_{c,i})}{\ln((T_{h,i} - T_{c,o}) / (T_{h,o} - T_{c,i}))}. \quad (5)$$

To minimize the surrounding heat loss, the difference between  $Q_c$  and  $Q_h$  was expressed as  $Q_{loss}$ :

$$Q_{loss} = Q_h - Q_c. \quad (6)$$

A negligible  $Q_{loss}$  of 4.72% was reported.

The average heat transfer between the cold and hot fluid ( $Q_{ave}$ ) was estimated according to the following equation:

$$Q_{ave} = \frac{Q_h + Q_c}{2}. \quad (7)$$

Based on the  $Q_{ave}$  value obtained from Equation (7), the overall heat-transfer coefficient of the inner tube ( $U_i$ ) was expressed as

$$Q_{ave} = U_i A_i \Delta T_{LMTD}. \quad (8)$$

Therefore, the convective heat-transfer coefficient in the inner tube ( $h_i$ ) was calculated using the following equation:

$$h_i = \frac{1}{\left[ \frac{1}{U_i} - \frac{d_i \ln(d_o/d_i)}{2k_p} - \frac{d_i}{d_o h_o} \right]}. \quad (9)$$

The average Nusselt number ( $Nu$ ) based on the  $h_i$  was calculated using the following equation:

$$Nu_i = \frac{h_i d_i}{k_i}. \quad (10)$$

The inner diameter of the inner tube ( $d_i$ ) and thermo-physical properties of water at the bulk mean temperature of the inner tube ( $T_b$ ) were used to calculate the Reynolds number:

$$Re = \frac{\rho u d_i}{\mu}. \quad (11)$$

Given the representation of fluid flow as the friction factor ( $f$ ), the friction factor for a fully developed turbulent flow inside the tube was defined as

$$f = \frac{\Delta P}{(\rho u^2 / 2)(L / d_i)}. \quad (12)$$

To evaluate the effect of using DWTs and LS, a comparison of the enhanced heat transfer and friction factor improvement among DWTs, LS and plain tube under identical pumping power [18,19] is also performed. This comparison is denoted as the thermal performance factor of the system ( $\eta$ ) and is expressed as:

$$\eta = \frac{h_t}{h_o} \Big|_{pp} = \frac{Nu_t}{Nu_o} \Big|_{pp} = \left( \frac{Nu_t}{Nu_o} \right) \left( \frac{f_t}{f_o} \right)^{-\frac{1}{3}}. \quad (13)$$

Uncertainty analyses of non-dimensional parameters was performed based on ANSI/ASME (American National Standards Institute/American Society of Mechanical Engineers) [20] for determining errors in the measurement data. The uncertainty values for the Nusselt number, friction factor, and Reynolds number were  $\pm 7.15\%$ ,  $\pm 5.53\%$ , and  $\pm 6.62\%$ , respectively.

### 3. Results and Discussion

#### 3.1. Validation of the Plain Tube

A study of the plain tube (without insert) was conducted and used to validate the experimental methods. Validation was performed by comparing the experimental data with the predicted data obtained from the standard correlation. The average relative error method was employed to evaluate the results. The Nusselt number ( $Nu$ ) from the experimental data was evaluated by comparing with the standard correlation proposed by Petukhov and Gnielinski [21], whereas the friction factor ( $f$ ) was compared with the standard correlation proposed by Blasius [22]. Standard correlations were expressed as follows:

Nusselt number correlation from Petukhov

$$Nu = \frac{(f/8)RePr}{1.07 + 12.7(f/8)^{1/2}(Pr^{2/3} - 1)}, \quad (14)$$

for  $10^4 < Re < 5 \times 10^6$ .

Nusselt number correlation from Gnielinski

$$Nu = \frac{(f/8)(Re - 1000)Pr}{1 + 12.7(f/8)^{1/2}(Pr^{2/3} - 1)}, \quad (15)$$

for  $10^3 < Re < 5 \times 10^6$ .

Friction factor correlation from Blasius

$$f = 0.3164Re^{-0.25}, \quad (16)$$

for  $4 \times 10^3 < Re < 10^5$

Figures 4 and 5 compare the experimental data and the data obtained from the standard correlation estimation.

It is evident that the Nusselt number agrees well with the predicted results of the empirical correlations of Petukhov and Gnielinski with less than  $\pm 2.8\%$  and  $\pm 7.1\%$  deviation, respectively, and friction factor values agree with Blasius correlation with less than  $\pm 2.5\%$  deviation.

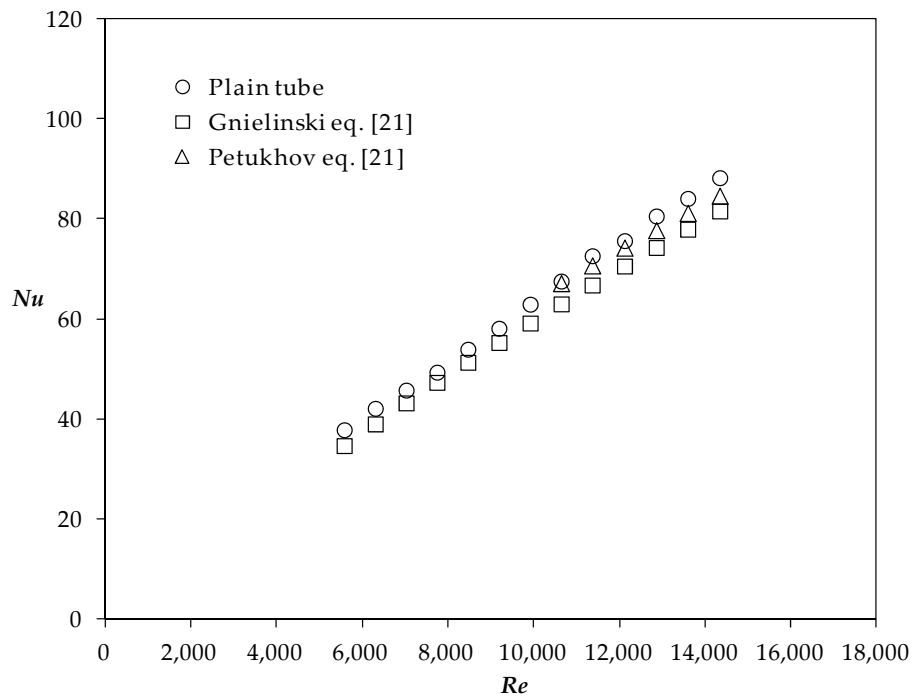


Figure 4. Validation of convective heat-transfer behavior of the plain tube.

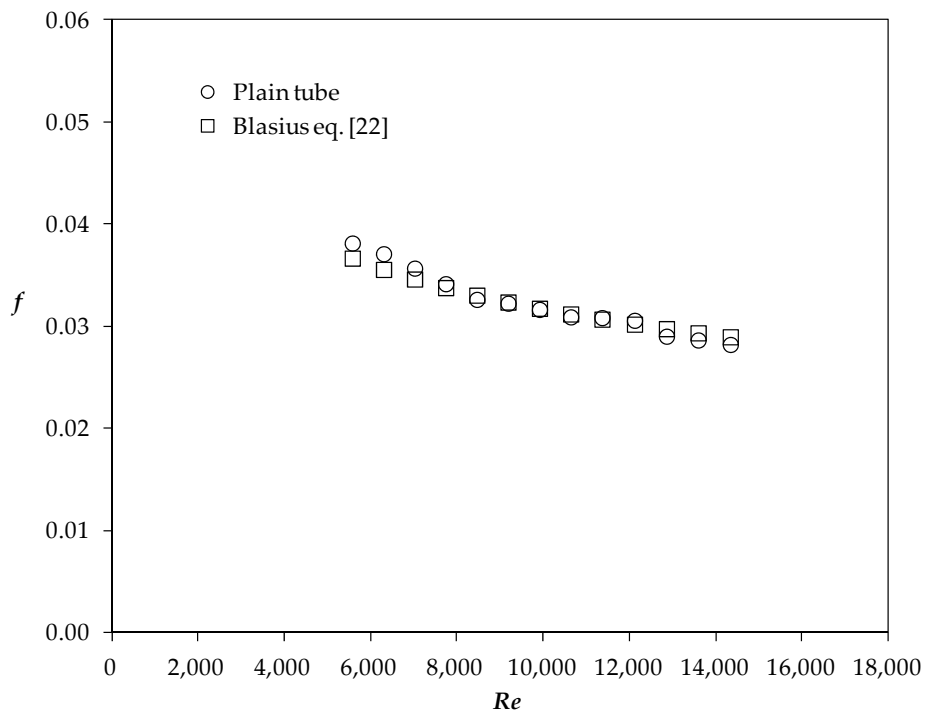
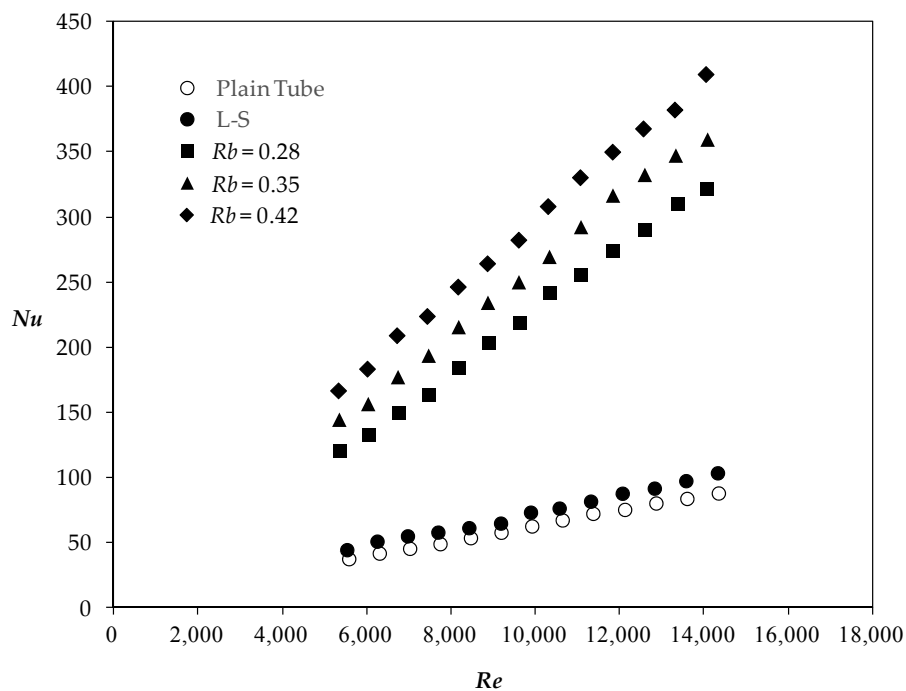


Figure 5. Validation of friction factor behavior of the plain tube.

### 3.2. Effect of Blockage Ratio on Heat-Transfer Behaviors

Figure 6 depicts the behavior of convective heat transfer in the value of Nusselt number ( $Nu$ ) plotted against Reynolds number ( $Re$ ) at the value of  $R_b = 0.28, 0.35,$  and  $0.42$  compared with LS and plain tube. Figure 6 shows that  $Nu$  increases as  $Re$  increases and confirms the results of our previous studies [16,23,24]. An increase in mean velocity, which increases the  $Re$ , leads to intensification of the

turbulence, thereby improving temperature gradients. This phenomenon significantly improved the heat-transfer rate [25]. The Nusselt numbers of the tube with DWT and LS insertions were higher than those of the plain tube. These insert devices placed in the path of the flow reduced the hydraulic diameter of the flow passage. Partitioning of the flow due to blockage raises the viscous level while diminishing the free-flow area and improves flow velocity [26]. Thus, better thermal contact and fluid mixing of the surface and the fluid at the core lead to a higher heat-transfer coefficient. Based on the data trend, DWTs show a higher  $Nu$ . The main mechanism that enhances heat transfer of DWTs is related to the presence of vortices. The wings of DWTs help create longitudinal vortices that lead to better mixing at a faster rate between the fluid at the core and the surface region and result in higher temperature gradients near the tube wall [27]. The alternating direction of DWTs also generated counter-rotating vortices, which induced additional convective thermal transport [5]. At the same time, these vortices produced a streamwise velocity profile, which led to decay of the flow. Together these factors contributed to the system's high heat-transfer coefficient. As is shown in Figure 6, a higher  $R_b$  produces a higher  $Nu$ . The higher  $R_b$  generated strong flow circulation and separation for higher turbulence intensity leading to higher heat-transfer performance [28]. The value of  $Nu$  in the inner tube with the addition of DWTs with  $R_b = 0.28, 0.35, 0.42$  and LS are increased in the ranges of 214.4–268.4%, 271.3–318.2%, 341.1–364.3%, and 10.8–17.84% compared with the  $Nu$  of plain tube, respectively.



**Figure 6.** Effect of blockage ratio ( $R_b$ ) on convective heat-transfer behavior ( $Nu$ ) with Reynolds number ( $Re$ ).

### 3.3. Effect of Blockage Ratio on Friction Factor

A friction factor analysis was conducted with an evaluation of the difference in pressure between the inlet and outlet of the test section. This pressure difference is associated with heat transfer which occurs at the surface. An assessment of the friction factor is not only based on the heat transfer but also based on the flow length of the heat exchange, the free-flow area, and the hydraulic diameter of the passage [29]. Figure 7 shows the influence of the blockage ratio ( $R_b$ ) on the friction factor ( $f$ ) as a function of the Reynolds number ( $Re$ ). A downtrend in  $f$  corresponds to an increase in  $Re$  number for all test conditions. These results are consistent with those reported in the authors' earlier publications [16,23,24]. As shown in Figure 7, the friction factor of the tube with DWT or LS insertions is higher than with the plain tube. When turbulent disturbance and core main flow increased, the

flow friction factor also increased. In addition, the blockage effect due to the thickness of the inserts significantly improved the flow friction factor [30]. The average friction factor in the inner tube with the addition of the DWT with  $R_b = 0.28, 0.35,$  and  $0.42$  increased by 11.8, 13.4, and 15.5, respectively, compared with the much lower friction factor values of the LS and plain tube, although the values of LS were slightly better those of the plain tube.  $R_b = 0.42$  showed the highest  $f$  value, which may be attributed to the increased surface area (solid-winglet/tape) that induced a larger recirculation zone behind the winglet, leading to higher vortex strength, higher turbulence intensity, and an enhanced friction factor [28].

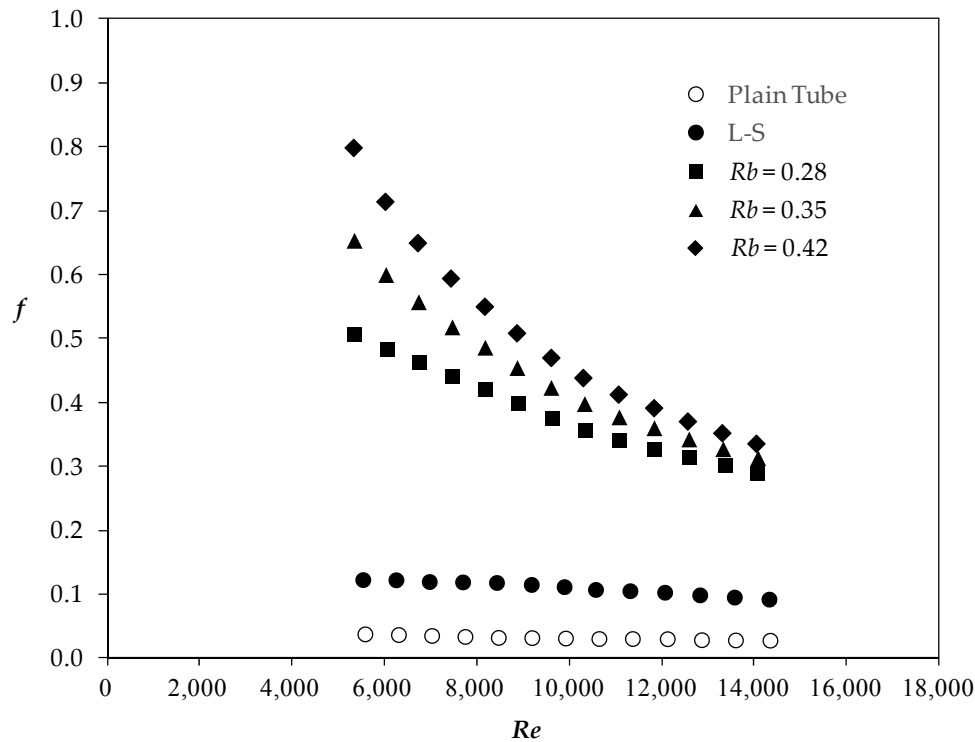


Figure 7. Effect of blockage ratio ( $R_b$ ) on the friction factor behavior ( $f$ ) with Reynolds number ( $Re$ ).

### 3.4. Effect of the Blockage Ratio on Thermal Performance

In general, the assessment of the enhancement of the heat transfer is done by calculating the thermal performance of the system. Figure 8 shows the effect of the blockage ratio ( $R_b$ ) on the thermal performance factor ( $\eta$ ) as a function of Reynolds number ( $Re$ ). The downward trend of  $\eta$  corresponds to the increasing  $Re$  for all test conditions.

Not all turbulators provide energy saving at high Reynolds numbers. The boundary layer of the heat exchanger directly influences thermal performance [26]. Any increase in the thickness of the boundary layer increases thermal resistance. This phenomenon mostly occurs in the laminar region or at a low Reynolds number. An increase in the Reynolds number because of increased flow velocity shrinks the boundary layer. A protuberance device such as a DWT is effectively disruptive at a low Reynolds number. The thermal performance of the heat exchanger with the addition of DWTs with  $R_b = 0.28, 0.35,$  and  $0.42$  and LS are in the ranges of 0.91–1.22, 0.96–1.30, 0.87–0.95, and 1.01–1.4, respectively.

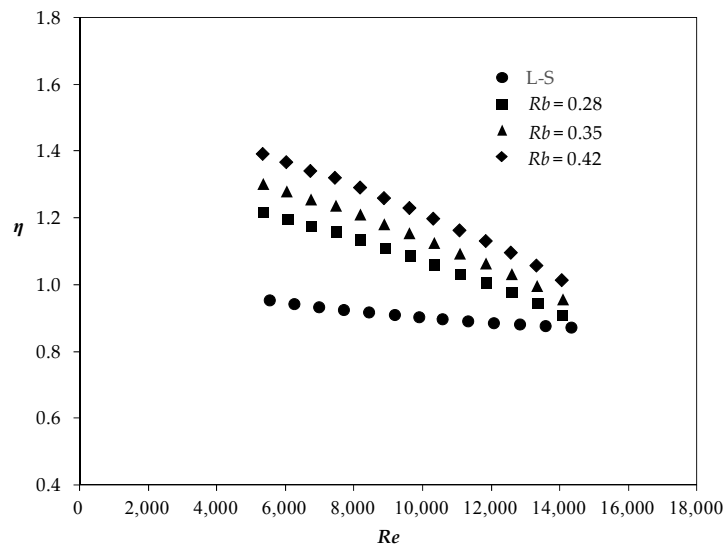


Figure 8. Effect of blockage ratio ( $R_b$ ) on the thermal performance factor ( $\eta$ ) with Reynolds number ( $Re$ ).

### 3.5. The Development of the Empirical Correlations

As shown below, three empirical correlations for non-dimensional parameters were developed using the following independent variables: Reynolds number ( $Re$ ) ranging from 5500 to 14,500, Prandtl number ( $Pr$ ) at 0.3 for cooling, and blockage ratio ( $R_b$ ) at 0.28, 0.35, and 0.42.

$$Nu = 0.037 Re^{0.995} Pr^{0.3} R_B^{0.639}, \tag{17}$$

$$f = 1098.424 Re^{-0.775} R_B^{0.72}, \text{ and} \tag{18}$$

$$\eta = 23.811 Re^{-0.297} R_B^{0.307}, \tag{19}$$

A plot of the predicted data derived from the empirical correlations is compared with the plots of experimental results, as shown in Figures 9–11. For all conditions, the relative deviation between the experimental data and predictive data were  $\pm 4.36\%$  for the Nusselt number ( $Nu$ ),  $\pm 7.48\%$  for the friction factor ( $f$ ), and  $\pm 3.47\%$  for the thermal performance factor ( $\eta$ ). It is evident that there is a close correlation between the predicted and empirical results.

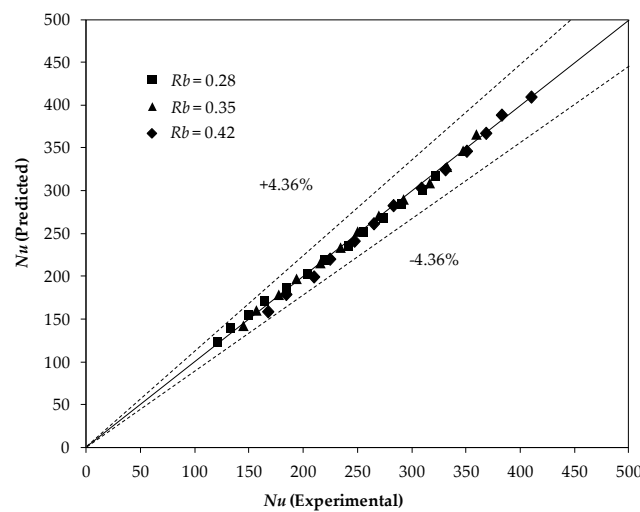


Figure 9. Comparison between the experimental  $Nu$  with predicted  $Nu$ .

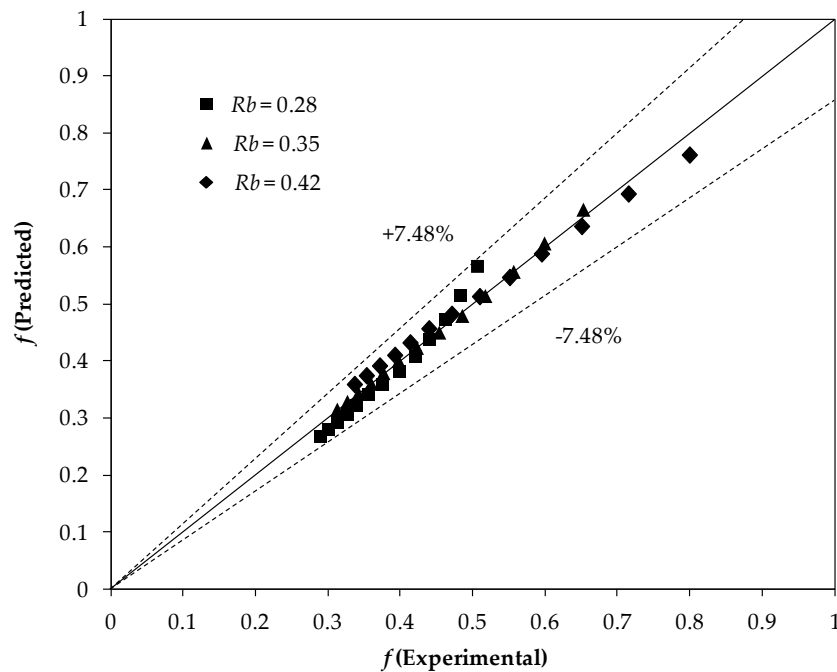


Figure 10. Comparison between the experimental  $f$  with predicted  $f$ .

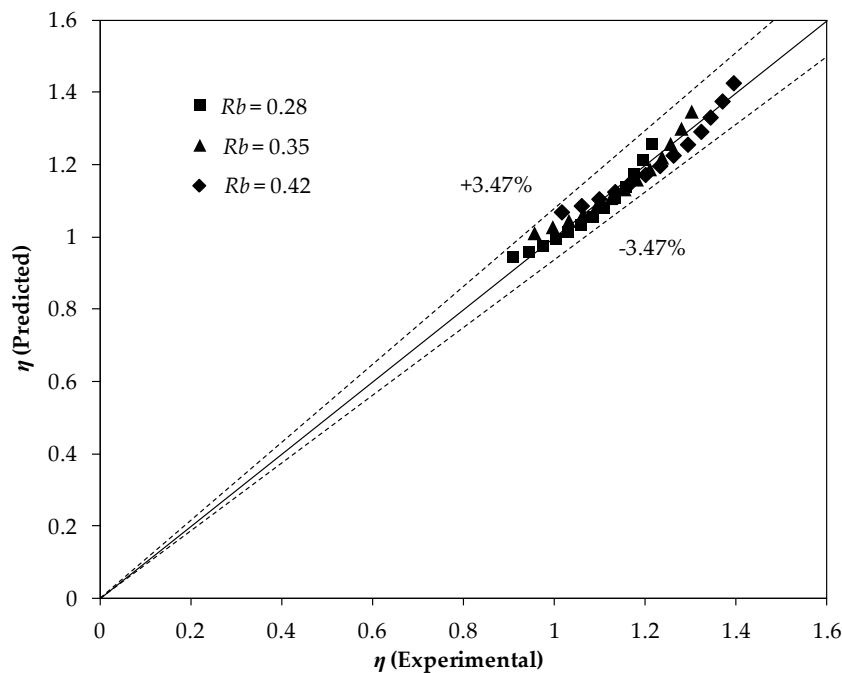


Figure 11. Comparison between the experimental  $\eta$  with predicted  $\eta$ .

#### 4. Conclusions

The performance of double-sided DWT VGs was experimentally investigated and compared with that of the LS and plain tube VGs. The conclusions drawn are as follows. The presence of DWTs yields a higher heat-transfer rate, friction factor, and thermal performance factor than the presence of the LS and plain tube. Thermal performance increased with an increase in the  $R_b$  of the DWT. The DWT with an  $R_b$  of 0.42 outperformed the other DWTs with a lower  $R_b$  in terms of heat-transfer rate, friction factor, and thermal performance factor. DWTs performed the best thermo-hydraulic performance in

low  $Re$ , whereas its performance decreased with a higher  $Re$ . There was high correlation between the experimental and predictive data with a relative deviation of  $\pm 4.36\%$  for the Nusselt number,  $\pm 7.5\%$  for friction, and  $\pm 3.47\%$  for thermal performance.

**Acknowledgments:** The first author wishes to thank the Ministry of Research, Technology, and Higher Education (RISTEKDIKTI) and the Ministry of Finance, Indonesia Endowment Fund for Education (LPDP) of the Republic of Indonesia, for their support of this study within the framework of BUDI-LN. The authors wish to thank their former colleague, Adi Eka Pranata, for his assistance during the experiments.

**Author Contributions:** Indri Yaningsih, Agung Tri Wijayanta, Takahiko Miyazaki and Shigeru Koyama conceived the main concept and contributed the analysis. Indri Yaningsih performed the experiments and wrote the paper. All authors contributed in writing the final manuscript.

**Conflicts of Interest:** The authors declare no conflict of interest.

## Nomenclature

$A_i$	inner surface area of the inner tube ( $m^2$ )
$A_o$	outer surface area of the inner tube ( $m^2$ )
$b$	winglet height (m)
$c$	winglet width (m)
$C_p$	specific heat capacity ( $J/kg \cdot K$ )
$d_i$	inner diameter of the inner tube (m)
$d_o$	outer diameter of the inner tube (m)
$D_i$	inner diameter of the outer tube (m)
$D_o$	outer diameter of the outer tube (m)
$f$	friction factor (dimensionless)
$f_t$	friction factor of the inner tube with DWTs (dimensionless)
$f_o$	friction factor of the plain tube (dimensionless)
$h_i$	average convective heat-transfer coefficient of the inner tube side ( $W/m^2 \cdot K$ )
$h_o$	average convective heat-transfer coefficient of the annulus side ( $W/m^2 \cdot K$ )
$h_p$	average convective heat-transfer coefficient of the plain tube ( $W/m^2 \cdot K$ )
$h_t$	average convective heat-transfer coefficient of the inner tube with T-Ws ( $W/m^2 \cdot K$ )
$k_i$	thermal conductivity of hot water ( $W/m \cdot K$ )
$k_p$	thermal conductivity of the inner tube material ( $W/m \cdot K$ )
$L$	length of the inner tube (m)
$Nu_o$	average Nusselt number of the plain tube (dimensionless)
$Nu_i$	average Nusselt number of the inner tube side (dimensionless)
$Nu_t$	average Nusselt number of the inner tube side with T-Ws (dimensionless)
$Nu_p$	average Nusselt number of the plain tube (dimensionless)
$P$	wing-pitch (m)
$Pr$	Prandtl number (dimensionless)
$Q_h$	heat-transfer rate from the hot water in the inner tube (Watt)
$Q_c$	heat transfer to the cold water in the annulus (Watt)
$R_b$	blockage ratio (dimensionless)
$Re$	Reynolds number (dimensionless)
$T_b$	bulk water temperature (K)
$T_c$	cold water temperature (K)
$T_h$	hot water temperature (K)
$T_w$	outer wall inner tube temperature (K)
$u$	velocity of hot water in the inner tube (m/s)
$U_i$	overall heat-transfer coefficient based on the inner tube inside surface area ( $W/m^2 \cdot K$ )
$\dot{V}$	volumetric flow rate of fluid ( $m^3/s$ )
$W$	aluminum strip width (m)

## Greek symbol

$\alpha$	slant angle ( $^\circ$ )
$\rho$	density of hot water ( $kg/m^3$ )

$\mu$	dynamic viscosity of hot water (kg/m·s)
$\eta$	thermal performance factor (dimensionless)
$\Delta P$	pressure drop across the inner tube (Pa)
$\Delta T_{LMTD}$	logarithmic mean temperature difference (K)

### Subscripts

<i>ave</i>	average
<i>c</i>	cold
<i>h</i>	hot
<i>i</i>	inlet
<i>o</i>	outlet

### References

1. Torii, K.; Yanagihara, J.I. The effect of longitudinal vortices on heat transfer of laminar boundary layers. *JSME Int. J.* **1989**, *32*, 395–402. [[CrossRef](#)]
2. Yanagihara, J.I.; Torii, K. Enhancement of laminar boundary layer heat transfer by a vortex generator. *JSME Int. J.* **1992**, *35*, 400–405. [[CrossRef](#)]
3. Fiebig, M.; Valencia, A.; Mitra, N.K. Local heat transfer and flow losses in fin-and-tube heat exchangers with vortex generators: A comparison of round and flat tubes. *Exp. Therm. Fluid Sci.* **1994**, *8*, 35–45. [[CrossRef](#)]
4. Jacobi, A.M.; Shah, R.K. Heat transfer surface enhancement through the use of longitudinal vortices: A review of recent progress. *Exp. Therm. Fluid Sci.* **1995**, *11*, 294–309. [[CrossRef](#)]
5. Fiebig, M. Vortices, generators, and heat transfer. *Chem. Eng. Res. Des.* **1998**, *76*, 108–123. [[CrossRef](#)]
6. Ferrouillat, S.; Tochon, P.; Garnier, C.; Peerhossaini, H. Intensification of heat transfer and mixing in multifunctional heat exchangers by artificially generated streamwise vorticity. *Appl. Therm. Eng.* **2006**, *26*, 1820–1829. [[CrossRef](#)]
7. Biswas, G.; Chattopadhyay, H.; Sinha, A. Augmentation of heat transfer by creation of streamwise longitudinal vortices using vortex generators. *Heat Transfer Eng.* **2012**, *33*, 406–424. [[CrossRef](#)]
8. Wu, J.M.; Tao, W.Q. Effect of longitudinal vortex generator on heat transfer in rectangular channels. *Appl. Therm. Eng.* **2012**, *37*, 67–72. [[CrossRef](#)]
9. He, Y.; Chu, P.; Tao, W.; Zhang, Y.; Xie, T. Analysis of heat transfer and pressure drop for fin-and-tube heat exchangers with rectangular winglet-type vortex generators. *Appl. Therm. Eng.* **2013**, *61*, 770–783. [[CrossRef](#)]
10. Gholami, A.A.; Wahid, M.A.; Mohammed, H.A. Heat transfer enhancement and pressure drop for fin-and-tube compact heat exchangers with wavy rectangular winglet-type vortex generators. *Int. Commun. Heat Mass Transf.* **2014**, *33*, 132–140. [[CrossRef](#)]
11. Khoshvaght-Aliabadi, M.; Sartipzadeh, O.; Alizadeh, A. An experimental study on vortex-generator insert with different arrangements of delta-winglets. *Energy* **2015**, *82*, 629–639. [[CrossRef](#)]
12. Wang, W.; Bao, Y.; Wang, Y. Numerical investigation of a finned-tube heat exchanger with novel longitudinal vortex generators. *Appl. Therm. Eng.* **2015**, *86*, 27–34. [[CrossRef](#)]
13. Abdollahi, A.; Shams, M. Optimization of shape and angle of attack of winglet vortex generator in a rectangular channel for heat transfer enhancement. *Appl. Therm. Eng.* **2015**, *81*, 376–387. [[CrossRef](#)]
14. Skullong, S.; Promvong, P.; Thianpong, C.; Pimsarn, M. Thermal performance in solar air heater channel with combined wavy-groove and perforated-delta wing vortex generators. *Appl. Therm. Eng.* **2016**, *100*, 611–620. [[CrossRef](#)]
15. Sarangi, S.K.; Mishra, D.P. Effect of winglet location on heat transfer of a fin-and-tube heat exchanger. *Appl. Therm. Eng.* **2017**, *116*, 528–540. [[CrossRef](#)]
16. Wijayanta, A.T.; Istanto, T.; Kariya, K.; Miyara, A. Heat transfer enhancement of internal flow by inserting punched delta winglet vortex generators with various attack angles. *Exp. Therm. Fluid Sci.* **2017**, *87*, 141–148. [[CrossRef](#)]
17. Honda, H.; Wijayanta, A.T.; Takata, N. Condensation of R407C in a horizontal microfin tube. *Int. J. Refrig.* **2005**, *28*, 203–211. [[CrossRef](#)]
18. Yakut, K.; Sahin, B. The effect of vortex characteristics on performance of coiled wire turbulators used for heat transfer augmentation. *Appl. Therm. Eng.* **2004**, *24*, 2427–2438. [[CrossRef](#)]

19. Yakut, K.; Sahin, B.; Canbazoglu, S. Performance and flow-induced vibration characteristics for conical ring turbulators. *Appl. Energy* **2004**, *79*, 65–76. [[CrossRef](#)]
20. ANSI/ASME. *Measurement Uncertainty*; PTC 19. 1 Part I; The American Society of Mechanical Engineers: New York, NY, USA, 1986.
21. Cengel, Y.A. *Heat and Mass Transfer*, 5th ed.; McGraw-Hill: New York, NY, USA, 2008.
22. White, F.M. *Fluid Mechanics*, 7th ed.; McGraw-Hill: New York, NY, USA, 2011.
23. Yaningsih, I.; Wijayanta, A.T. Concentric Tube Heat Exchanger Installed by Twisted Tape Using Various Wings with Alternate Axis. In Proceedings of the AIP Conference, Solo, Indonesia, 3–5 August 2016.
24. Yaningsih, I.; Istanto, T.; Wijayanta, A.T. Experimental Study of Heat Transfer Enhancement in a Concentric Double Pipe Heat Exchanger with Different Axial Pitch Ratio of Perforated Twisted Tape Inserts. In Proceedings of the AIP Conference, Solo, Indonesia, 11–12 November 2015.
25. Razgaitis, R.; Holman, J.P. A survey of heat transfer in confined swirl flows. *Heat Mass Transf. Proc.* **1976**, *2*, 831–866.
26. Saha, S.K.; Tiwari, M.; Sundén, B.; Wu, Z. *Advances in Heat Transfer Enhancement*; Springer: Basel, Switzerland, 2016.
27. Eiamsa-ard, S.; Promvong, P. Influence of double-sided delta-wing tape insert with alternate-axes on flow and heat transfer characteristics in a heat exchanger tube. *Chin. J. Chem. Eng.* **2011**, *19*, 410–423. [[CrossRef](#)]
28. Skullong, S.; Promvong, P.; Thianpong, C.; Jayranaiwachira, N. Thermal behaviors in a round tube equipped with quadruple perforated-delta-winglet pairs. *Appl. Therm. Eng.* **2017**, *115*, 229–243. [[CrossRef](#)]
29. Shah, R.K.; Sekulić, D.P. *Fundamentals of Heat Exchanger Design*; John Wiley & Sons, Inc.: Hoboken, NJ, USA, 2003.
30. Hsieh, S.; Wu, F.; Tsai, H. Turbulent heat transfer and flow characteristics in a horizontal circular tube with strip-type inserts. Part I. Fluid Mechanics. *Int. J. Heat Mass Transf.* **2003**, *46*, 837–849. [[CrossRef](#)]



© 2018 by the authors. Licensee MDPI, Basel, Switzerland. This article is an open access article distributed under the terms and conditions of the Creative Commons Attribution (CC BY) license (<http://creativecommons.org/licenses/by/4.0/>).